Journal of Materials Chemistry A

Accepted Manuscript

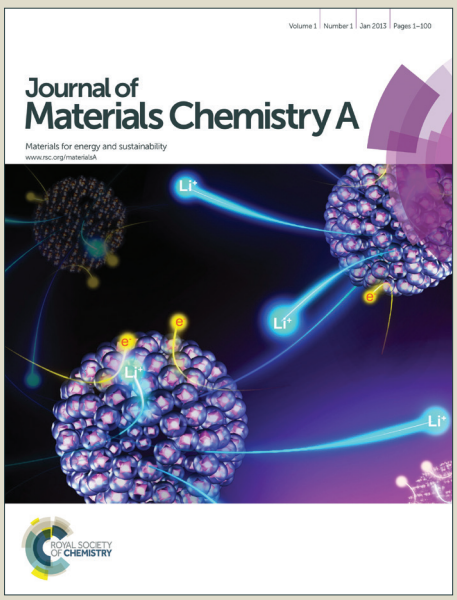

ROYAL SOCIETY OF CHEMISTRY

www.rsc.org/materialsA

Bioinspired Underwater Superoleophobic Surface with Ultralow Oil-Adhesion Achieved by Femtosecond Laser Microfabrication

Jiale Yong, Feng Chen, Qing Yang, Dongshi Zhang, Umar Farooq, Guangqing Du and Xun Hou*

State Key Laboratory for Manufacturing System Engineering & Key Laboratory of Photonics Technology for Information of Shaanxi Province, School of Electronics & Information Engineering, Xi'an Jiaotong University, Xi'an, 710049, P. R. China

E-mail address: *chenfeng@mail.xjtu.edu.cn.

Femtosecond laser microfabrication has been recently utilized in interface science to modify the liquid wettability of solid surfaces. In this paper, silicon surface with hierarchical micro/nanostructure is fabricated by a femtosecond laser. Similar to the fish's scales, the laser-induced surface shows superhydrophilicity in air and superoleophobicity underwater. The oil contact angles can reach up to 159.4 ± 1° and 150.3 ± 2° for the 1,2-dichloroethane and chloroform droplets in water. Besides, the surface exhibits ultralow oil-adhesion. In the oil/water/solid three-phase system, water can be trapped in the hierarchical rough structure and forms a repulsive oil layer according to extended Cassie's theory. The contact area between the as-prepared surface and oil droplet is significantly reduced, resulting in superoleophobicity and ultralow oil-adhesion in water. In addition, as a potential application, the working principle diagram of preventing blockage ability of underwater superoleophobic pipes is first propounded.

1. Introduction

Wettability is a very important property of solid surfaces that is governed by both the geometrical microstructure and the chemical composition of the materials.[1-9] Superhydrophobic surface, displaying a water contact angle (WCA) greater than 150°, is initially observed from natural materials such as lotus leaf.[10,11] The lotus leaf surface is found to be completely covered by many micro/nanoscale hierarchical papillas and an additional layer of hydrophobic wax crystals.[12-16] The combined action can minimize the real contact area between the surface and the droplet, leading to great enhancement of the superhydrophobicity. Inspired by the lotus leaf, artificial

superhydrophobic surfaces have been designed in large numbers and widely used in many fields, for instance, in the areas of surface self-cleaning, marine coating, preventing the adhesion of snow, fog and raindrops to window surfaces and reducing flow resistance in microfluidic channels.[17-23] Oil, another common liquid in our daily life, is most often selected as the research object recently to investigate the interface of solid and liquid.[24-31] Following superhydrophobic surface, the superoleophobicity can be characterized by oil contact angle (OCA) larger than 150°.

It is well-known that fishes can swim freely under water and keep their scales clean even in the oil-polluted water when the accident of oil spill is happened.[32,33] Recently, Jiang et al. revealed that this remarkable ability is ascribed to the special underwater superoleophobicity of fish's scales.[34,35] The combination of the hierarchical rough structures and hydrophilic chemistry of the fish scales gives rise to the underwater superoleophobicity. According to Cassie's theory, an air layer can be trapped in the water-solid interface when a water droplet is placed on a rough solid surface with low surface energy in air environment.[36] It provides a water-air-solid interface that reduces the contact area between water and solid, leading to a high WCA. Air is an ideal water repellent material because a small water droplet suspending in the air is spherical.[37] For the same reason, water is an excellent oil repellent material. Similar to the role of air layer for achieving superhydrophobicity, if water fills between the hierarchical rough structures of solid surface, a water layer can form in the oil-solid interface. Water layer can improve the oleophobicity in an oil-water-solid interface, which may provide the possibility for fabricating underwater superoleophobic surfaces.[34,35] Taking the inspiration of these findings, lots of underwater superoleophobic materials have been prepared.[27] These novel materials show some fantastic practical applications, such as preventing blockage, bio-adhesion, microfluidic technology, and oil/water separation.[38-43] However, most reported methods used to fabricate underwater superoleophobic surfaces generally require complex fabrication processes, and have tight restrictions on materials, and are lack of flexibility. It is still expected to explore a versatile and simple way to realize underwater superoleophobicity.

In recent years, micromachining by femtosecond laser has been utilized in interface science to modify the liquid wettability of solid surfaces.[44-51] This technology has many distinct advantages, such as negligible heat-affected zone, precise ablation threshold and high resolution.[44,50] Moreover, this method can be applied to a wide variety of materials such as metals, glasses, ceramics and polymers.[52-55] A two scale rough microstructure can be easily built by femtosecond laser scanning. Controlled by a computer, femtosecond laser micromachining provides a quick and efficient prototyping means which can control the processing position precisely being independent of expensive masks and clean room. Various patterns can be realized, exhibiting unique wetting property. Although this technology has been a great success in achieving superhydrophobic surfaces, to the best of our knowledge, the fabrication of superoleophobic surfaces via a femtosecond laser is still scarce.

In this paper, we present an effective method to prepare underwater superoleophobic surface by femtosecond laser microfabrication on silicon in ambient

environment. After irradiating by femtosecond laser pulses through a line-by-line and serial scanning process, the sample surface shows a micro/nanoscale hierarchical spike forest structure. The hierarchical surface of high roughness exhibits extreme underwater superoleophobicity, with OCAs greater than 150° for the 1,2-dichloroethane and chloroform droplets in water. The adhesion between the as-prepared surface and oil droplet is very low that the oil droplets can move easily even when the surface is only slightly titled. In addition, as a potential application, we make an attempt to put forward the working principle diagram of preventing blockage ability of underwater superoleophobic surface.

2. Experimental Section

The micro/nanoscale hierarchical structure was prepared by femtosecond laser irradiation in air atmosphere on flat silicon surface through a line-by-line and serial scanning process. The schematic of the experimental setup was shown in our previous work.[45-51] A single crystal p-type Si (100) wafer with thickness of 0.5 mm was used. The sample was mounted on a motorized x–y–z translation stage controlled by a computer, and then irradiated by a regenerative amplified Ti:sapphire laser system (center wavelength: 800 nm; pulse duration: 50 fs; repetition: 1 kHz) (CoHerent, Libra-usp-1K-he-200). The Gaussian laser beam was focused by a microscope objective lens (20×, NA= 0.45, Nikon) on the front side of the sample. The laser energy is 20 mW and the scanning speed was 2 mm/s. The interval of adjacent laser scanning lines was set at 2 μm. Since the laser repetition rate was 1 kHz, the adjacent distance of laser pulse focuses was 2 μm. Following the irradiation process, the sample was successively cleaned by acetone, alcohol, and deionized water in ultrasonic bath for 10 minutes each time.

The morphology of the as-prepared surfaces irradiated by a femtosecond laser was characterized by a JSM-7000F scanning electron microscopy (SEM, JEOL, Japan). The contact angles of an 8 μl water or oil droplet on the surface were measured by a JC2000D4 contact-angle system (POWEREACH, China). In the water contact angle test, the sample was placed on a sample stage. In the underwater oil contact angle test, the sample was put in a homemade sink filled with deionized water. For detecting oils, 1,2-dichloroethane ($C_2H_4Cl_2$) and chloroform ($CHCl_3$) were used. The average values were obtained by measuring five different points on the same surface. The adhesion between the as-prepared surface and oil droplet in water was investigated by the contact-angle system and a charge-coupled device (CCD) camera system to take photographs at 25 frames per second.

3. Results and discussion

Figure 1 shows the typical SEM images of the femtosecond laser-induced structure. The morphology is characterized by self-organized conical spike forest with period of 10 μm. Each spike is decorated with tens or a few hundreds of nanometer-sized protrusions. The micro/nanoscale hierarchical structure is highly uniform. The

formation of this structure is considered to evolve from the microscale ridges.[37,51,56,57] The average diameter of the periodic conical spikes is about 6 μm, and the height is 2.9 μm (Figure 1d). Every conical spike is surrounded by four microscale holes. The average diameter and depth of the holes are about 8 and 4.6 μm, respectively. As a result, the distance from the top of the spikes to the bottom of the holes can reach up to 7.5 μm, resulting in a significant increase in the overall roughness. The surface roughness (R_a) is about 2.46 μm. This hierarchical rough structure is helpful to achieve superhydrophilicity in air and superoleophobicity in water.

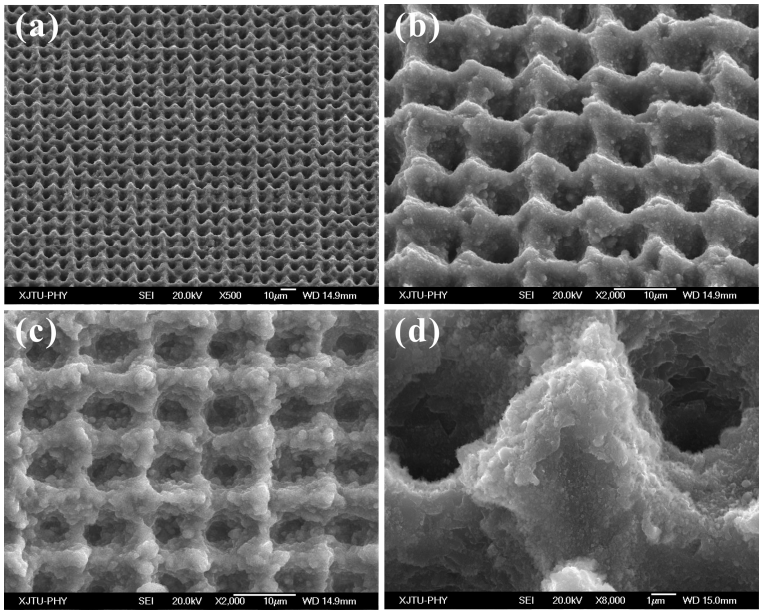

Figure 1. Typical SEM images of the structure irradiated by femtosecond laser. (a) 45° tilted view SEM image. (b) Higher resolution 45° tilted view SEM image. (c) Top view SEM image. (d) High magnification SEM image of a single spike decorating with nanoscale protrusions.

Previous studies have shown that the superhydrophilicity of a solid surface in air is crucial for realizing superoleophobicity in water.[27,34,35] When a water droplet is placed on a flat silicon surface in air, the WCA is about 60° (Figure 2a). In water, the shape of oil droplet is nearly half-sphere alike. The OCA is 124.6 ± 1° for an oil (1,2-dichloroethane) droplet, indicating the silicon wafer behaves as an commonly oleophobic surface in water (Figure 2c). After femtosecond laser irradiation, the as-prepared surface shows superhydrophilicity in air. When a water droplet is placed on the as-prepared surface, it can spread quickly, resulting in a contact angle of nearly 4° (Figure 2b). Figure 2d shows the image of an 8 μl oil droplet lying on the laser-induced surface in water. The oil droplet is an approximately spherical shape, and the OCA is as high as 159.4 ± 1° at this time, indicating underwater superoleophobicity.

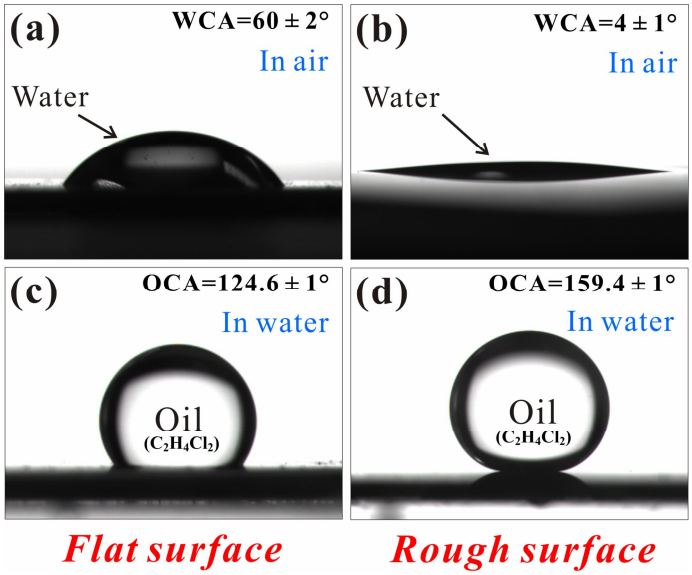

Figure 2. Comparison of the wetting properties of the surface before and after femtosecond laser treatment. (a,b) Shapes of a water droplet on the (a) flat surface and (b) rough surface in air, respectively. (c,d) Shapes of a 1,2-dichloroethane droplet on the (c) flat surface and (d) rough surface in water, respectively.

The average distance (D) of laser pulse focuses is a crucial machining parameter in our experiment, which is determined by the scanning speed and interval of adjacent laser scanning lines. A detailed definition of D can consult our previous work.[48] Figure 3 shows the dependence of the OCA on D. It can be seen that the OCA slowly decreases from 159.4 ± 1° to 156.7 ± 2.7° as D increases from 2 μm to 25 μm. A higher D has not been tested because it might damage the equipment. Clearly, this fluctuation is negligible and all the OCAs are higher than 150°, indicating that the underwater superoleophobicity can be realized in a wide technology parameter range. The result shows that the femtosecond laser microfabrication is useful and is an effective method for underwater superoleophobic surfaces.

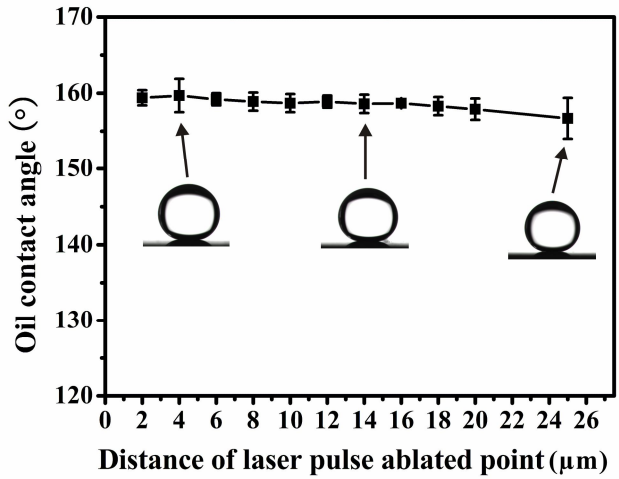

Figure 3. Dependence of the oil contact angle on the distance of laser pulse focuses.

The underwater oil-adhesion of the femtosecond laser structured surface was investigated by three usual means. As seen in Figure 4a and Movie S1 in Supporting

Information, a 6 µl oil (1,2-dichloroethane) droplet was first suspended on a microsyringe and then slowly lowered down. After the as-prepared surface making contact with the oil droplet, the microsyringe was lift up. Interestingly, the suspending oil droplet had difficulty falling on the structured surface; that is, in comparison to the large droplet, the surface adhesion was negligible even though the droplet was deformed severely by the downward pushing force produced during microsyringe decline. As the microsyringe was moved upward, the droplet would depart from the sample and be taken away. During the whole contacting and leaving process, the oil droplet kept nearly spherical shape all the time, and the oil droplet could be transferred away without loses, showing a ultralow oil-adhesion between the as-prepared surface and the oil droplet in water. The oil droplet could detach from the microsyringe and fall on the sample under the gravitation effect until the oil volume reached 8 µl. A similar process is described in Figure 4b and Movie S2 in Supporting Information. An oil droplet was dragged by the needle tip of microsyringe along the as-prepared surface freely. There was also no oil lose during the oil droplet going straight. The low oil-adhesion can be easily concluded following the process of Figure 4a.

The oil-adhesion can also be accurately assessed by the sliding behavior of an oil droplet. Interestingly, experimental results show that the oil droplet can move very easily even when the as-prepared surface are only slightly tilted or shaken. Figure 4c shows a time sequence of snapshots of an oil droplet rolling on a 0.5° tilted structured surface, indicating an ultralow adhesion between laser-induced surface and oil droplet in water (Movie S3 in Supporting Information). Before this, surfactant solution was traditionally used to reduce the adhesive force between oil droplets and solid surfaces, but these chemical substances are potentially contaminative to living environments []. In our experiment, the low oil-adhesion is highly dependent on the micro/nanostructures, which are considered to be environmentally friendly, instead of on the surfactants. Both the high OCA and the ultralow oil-adhesion demonstrate that the as-prepared surface has outstanding character of underwater superoleophobicity and dual-scale hierarchical structure is very important to enhance the oleophobicity of solid surface.

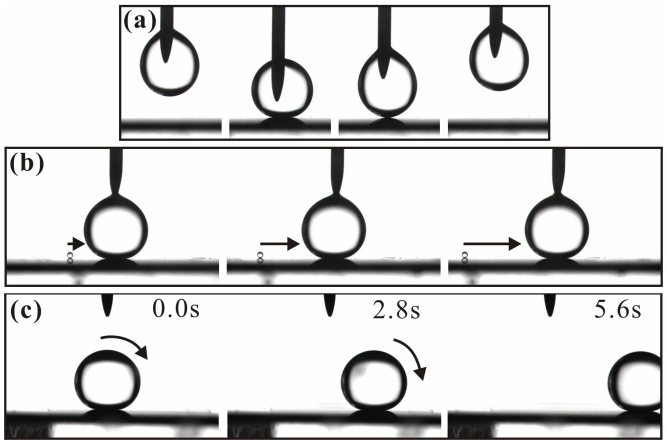

Figure 4. Oil-adhesion of the femtosecond laser structured surface. (a) Photographs of a 6 µl oil droplet contacting and leaving with the laser-induced surface. (b) Pulling an oil droplet on the laser-induced surface. The surface was

marked the location with an ultra-small liquid droplet (starting point of the black arrow) by spraying method before the experiment. (c) Time sequence of snapshots of an oil droplet rolling on the 0.5° tilted surface. 1,2-dichloroethane was used as detecting oil.

The underwater superoleophobicity and ultralow oil-adhesion can also be observed in the case of chloroform droplet. Figures 5a shows the shape of a chloroform droplet on the flat surface in water with OCA of 107.7 ± 1°. After femtosecond laser irradiation, the OCA has a significant increase, and the value reaches up to 150.3 ± 2° (Figure 5b). The OCA has met the requirement of superoleophobicity. When a chloroform droplet was placed on a 1° tilted structured surface, it would instantaneously roll off under the gravitation effect, as shown in Figure 5c and Movie S4 in Supporting Information. The sliding angle is very low, as well as the oil-adhesion between the laser-induced surface and chloroform droplet in water.

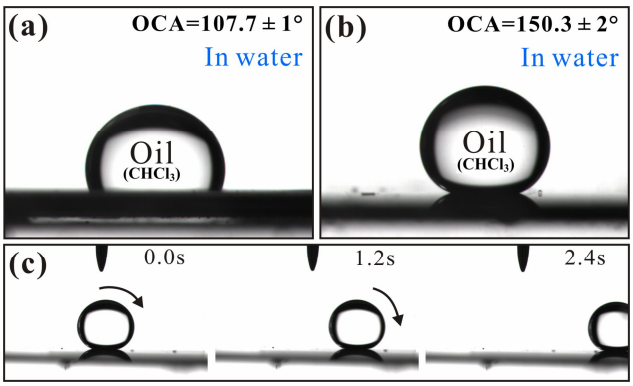

Figure 5. Superoleophobicity and ultralow oil-adhesion of the as-prepared surface. (a) Shape of a chloroform droplet on the flat surface. (b) Shape of a chloroform droplet on the as-prepared rough surface. (c) Time sequence of snapshots of a chloroform droplet rolling on the 1° tilted surface.

To well understand the underwater superoleophobicity of the femtosecond laser structured surface, the potential mechanism that has an influence on the oil contact angles was revealed. In air, the wettability of the solid surface is generally estimated by the contact angle according to Young's equation.[27,34,35] Although the equation is originally applied for a liquid droplet on a solid surface in air, it can be extended to a liquid droplet on a solid surface in the presence of a second liquid. For example, in the oil/water/solid three-phase system (Figure 6a), the OCA on a flat surface can be expressed by modified Young's equation:[27,34,35]

$$\cos\theta_{ow} = \frac{\gamma_{oa}\cos\theta_o - \gamma_{wa}\cos\theta_w}{\gamma_{ow}} \quad (1)$$

where γ_{oa}, γ_{wa}, and γ_{ow} are the oil-air interface tension, water-air interface tension, and oil-water interface tension, respectively. θ_o, θ_w, and θ_{ow} are the contact angles of oil in air, water in air, and oil in water, respectively. From Equation 1 we are able to obtain that a hydrophilic surface in air becomes oleophobic in water.[34]

After the introduction of micro/nanoscale hierarchical rough structure, a broad Cassie state can be achieved in the oil/water/solid system. When such surfaces are immersed into water, water can enter into the microstructures easily and occupy the whole interspaces between the microstructure on the surfaces, and be trapped among the micro/nanostructures. The oil droplet will reside on a composite solid-water interface, forming an oil/water/solid system, as shown in Figure 6b. The water, which is filled in the interspaces between the oil droplet and the as-prepared surface, is an ideal superoleophobic material and results in the underwater superoleophobicity. The high oil contact angle can be explained by the generalized Cassie's equation:[32,33]

$$\cos\theta^*_{ow} = f\cos\theta_{ow} + f - 1 \quad (2)$$

where f is the area fraction of the projected oil wet area, θ_{ow} is the oil contact angle on a flat surface in water, and θ^*_{ow} is the contact angle of an oil droplet on a rough surface in water. In our experiment, the θ_{ow} was measured to be 124.6 ± 1° when an 1,2-dichloroethane droplet was in contact with flat silicon in water. For the femtosecond laser structured surface, the oil droplet only contacts a small area of the surface, and the value of f can be inferred to be about 0.111 according to our previous work.[37] Therefore, we can calculate θ^*_{ow} according to Equation 2 and the value is close to 162° for 1,2-dichloroethane droplet. The theoretical calculation agrees well with the measured value. Using the same manner, the calculated value of θ^*_{ow} of a chloroform droplet is about 157°, fitting our experimental result very well. According to the Cassie's model, oil droplet sits on the conical spike forest, and water is trapped below the oil droplet. The water trapped in the hierarchical rough structure is a repulsive liquid phase for oil, giving rise to superoleophobic property. On the other hand, the hierarchical microstructure can effectively reduce the contact area between the silicon surface and the oil droplet. As a result, the as-prepared surface shows small adhesive force and ultralow oil adhesion. From the above analysis, it is concluded that hydrophilicity in air results in underwater oleophobicity, whereas the hierarchical rough structure can significantly amplify the superoleophobicity.

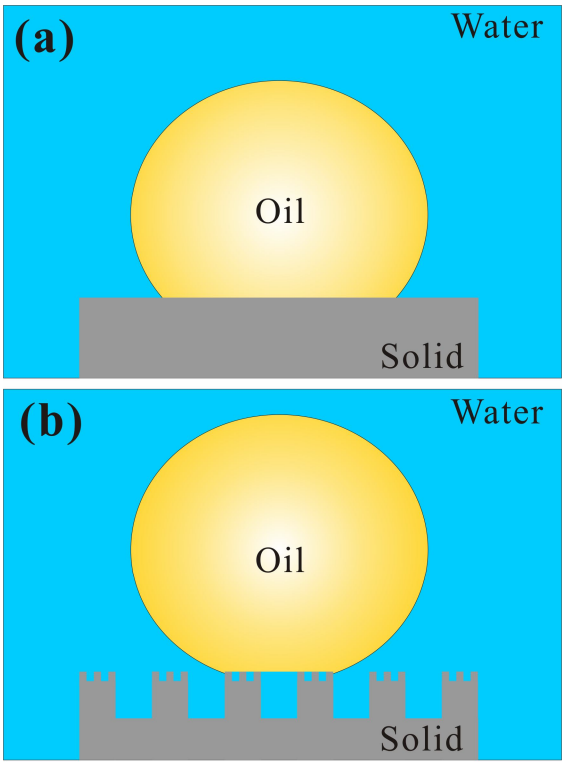

Figure 6. Diagrams illustrate the effect of surface structure on the wetting behavior of solid substrates in oil/water/solid three-phase system. An oil droplet on (a) flat surface and (b) micro/nanostructured surface in water phase.

The water mixing with oil impurity is common in the pipes of household kitchenware, and the drainage pipes are often blocked by the oil kind dirt. At present, the underwater superoleophobic surface with ultralow oil-adhesion provides a promising way to solve this problem. Figure 7a shows the schematic of water with oil impurity flowing in a conventional pipe. Because of large contact area between oil and pipe surface, which results in a high oil-adhesion, the oil impurity may stick closely to the inner wall of the pipe. On the one hand, the adherent oil droplet changes the movement tendency of the water. The speed of water flow will diminish significantly for proceeding in an irregular course, making draining away water less efficient. On the other hand, the adherent oil droplet can contact with other free oil impurity and forms a larger one. After some time, the adherent oil accumulates at a certain level and it will block the pipe. The blockage of drainage pipes will draw a lot of inconveniences and problems to our daily life. However, if the inner wall of the pipe shows superoleophobicity and ultralow oil-adhesion, the oil impurity droplet will roll forward along with the flow of water, as shown in Figure 7b. In this way, the oil impurity's influence to the movement tendency of water attains minimum, and the drainage pipes can keep high-performance for an extended period of time. The oil-induced blockage is prevented for the impurity being taken away in time. This anti-blocking function can also be widely used in other fields, such as tissue engineering, etc. If the artificial blood vessels possess underwater superoleophobicity, the

occurrence probability of vascular obstruction will greatly reduce.

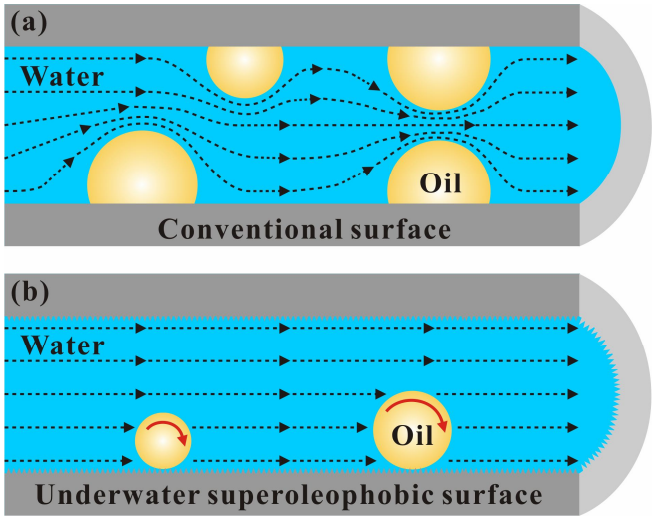

Figure 7. Schematics of the effect of underwater superoleophobic surface on preventing water pipe blocking by oil impurity. (a) Water with oil impurity flows in a conventional pipe. (b) Water with oil impurity flows in an underwater superoleophobic pipe. The black dotted lines express the movement tendency of the water. The red arrows indicate that the oil impurity droplet can roll forward along with the flow of water.

5. Conclusions

In summary, inspired by the fish's scales, the underwater superoleophobic surface was fabricated by a femtosecond laser on silicon. The laser-induced surface shows micro/nanoscale hierarchical structure. The oleophobic properties of the as-prepared surface and underlying mechanisms are systematically investigated. The oil contact angles can reach up to 159.4 ± 1° and 150.3 ± 2° for the 1,2-dichloroethane and chloroform droplets in water. In addition, the surface shows ultralow oil-adhesion. The sliding angles are only about 0.5° and 1° for the 1,2-dichloroethane and chloroform droplets. In the oil/water/solid three-phase system, water can be trapped in the hierarchically rough structures and forms a repulsive oil layer. The contact area between the as-prepared surface and the oil droplet is significantly reduced, resulting in the superoleophobicity and low oil-adhesion in water. The presented method is simple and can accurately control the processing location, which may have widely potential applications in, for instance, microfluidics, biotechnologies, and antifouling coatings.

ACKNOWLEDGMENTS

This work is supported by the National Science Foundation of China under the Grant Nos. 61275008 and 51335008, the Special-funded program on national key scientific instruments and equipment development of China under the Grant No.

2012YQ12004706.

References

(1) F. Xia and L. Jiang, *Adv. Mater.*, 2008, **20**, 2842-2858.
(2) T. L. Sun and G. Y. Qing, *Adv. Mater.*, 2011, **23**, H57-H77.
(3) K. S. Liu and L. Jiang, *Annu, Rev. Mater. Res.*, 2012, **42**, 231-263.
(4) K. S. Liu and L. Jiang, *Nano Today*, 2011, **6**, 155-175.
(5) X. Yao, Y. L. Song and L. Jiang, *Adv. Mater.*, 2011, **23**, 719-734.
(6) Y. L. Zhang, H. Xia, E. Kim, H. B. Sun, *Soft Matter*, 2012, **8**, 11217-11231.
(7) Y. L. Zhang, Q. D. Chen, Z. Jin, E. Kim and H. B. Sun, *Nanoscale*, 2012, **4**, 4858-4869.
(8) Y. B. Zhang, Y. Chen, L. Shi, J. Li and Z. G. Guo, *J. Mater. Chem.*, 2012, **22**, 799-815.
(9) X. F. Gao and L. Jiang, *Nature*, 2004, **432**, 36.
(10) X. Deng, L. Mammen, Y. Zhao, P. Lellig, K. Müllen, C. Li, H. J. Butt and D. Vollmer, *Adv. Mater.*, 2011, **23**, 2962-2965.
(11) Y. Li, L. Li and J. Q. Sun, *Angew. Chem.*, 2010, **122**, 6265-6269.
(12) W. Barthlott, C. Neinhuis, *Planta*, 1997, **202**, 1-8.
(13) V. Zorba, E. Stratakis, M. Barberoglou, E. Spanakis, P. Tzanetakis, S. H. Anastasiadis and C. Fotakis, *Adv. Mater.*, 2008, **20**, 4049-4054.
(14) J. L. Yong, Q. Yang, F. Chen, D. S. Zhang, G. Q. Du, J. H. Si, F. Yun and X. Hou, *J. Micromech. Microeng.*, 2014, **24**, 035006.
(15) Q. F. Cheng, M. Z. Li, Y. M. Zheng, B. Su, S. T. Wang and L. Jiang, *Soft Matter*, 2011, **7**, 5948.
(16) L. Feng, S. H. Li, Y. S. Li, H. J. Li, L. J. Zhang, J. Zhai, Y. L. Song, B. Q. Liu, L. Jiang and D. B. Zhu, *Adv. Mater.*, 2002, **14**, 1857-1860.
(17) T. K. Wong, S. H. Kang, S. K. Y. Tang, E. J. Smythe, B. D. Hatton, A. Grinthal and J. Aizenberg, *Nature*, 2011, **477**, 443-446.
(18) W. Barthlott, T. Schimmel, S. Wiersch, K. Koch, M. Brede, M. Barczewski, S. Walheim, A. Weis, A. Kaltenmaier, A. Leder H. F. Bohn, *Adv. Mater.*, 2010, **22**, 2325-2328.
(19) X. F. Gao, X. Yan, X. Yao, L. Xu, K. Zhang, J. H. Zhang, B. Yang and L. Jiang, *Adv. Mater.*, 2007, **19**, 2213-2217.
(20) M. Motornov, R. Sheparovych, R. Lupitskyy, E. MacWilliams and S. Minko, *Adv. Mater.*, 2008, **20**, 200-205.
(21) G. McHale, N. J. Shirtcliffe, C. R. Evans and M. I. Newton, *Appl. Phys. Lett.*, 2009, **94**, 064104.
(22) Y. K. Lai, Y. X. Tang, J. J. Gong, D. G. Gong, L. F. Chi, C. J. Lin and Z. Chen, *J. Mater. Chem.*, 2012, **22**, 7420-7426.
(23) N. J. Shirtcliffe, G. McHale, M. I. Newton and Y. Zhang, *ACS Appl. Mater. Interfaces*, 2009, **1**, 1316-1323.
(24) A. Tuteja, W. Choi, M. Ma, J. M. Mabry, S. A. Mazzella, G. C. Rutledge, G. H. McKinley and R. E. Cohen, *Science*, 2007, **318**, 1618-1622.

(25) X. Deng, L. Mammen, H. Butt and D. Vollmer, *Science*, 2012, **335**, 67-70.
(26) K. Li, Jie. Ju, Z. X. Xue, J. Ma, L. Feng, S. Gao and L. Jiang, *Nat. Commun.*, 2013, **4**, 2276.
(27) Z. X. Xue, Y. Z. Cao, N. Liu, L. Feng and L. Jiang, *J. Mater. Chem. A*, 2014, **2**, 2445-2460.
(28) Y. Huang, M. J. Liu, J. X. Wang, J. M. Zhou, L. B. Wang, Y. L. Song and L. Jiang, *Adv. Funct. Mater.*, 2011, **21**, 4436-4441.
(29) X. L. Liu, J. Zhou, Z. X. Xue, J. Gao, J. X. Meng, S. T. Wang and L. Jiang, *Adv. Mater.*, 2012, **24**, 3401-3405.
(30) L. P. Xu, J. Zhao, B. Su, X. L. Liu, J. T. Peng, Y. B. Liu, H. L. Liu, G. Yang, L. Jiang, Y. Q. Wen, X. J. Zhang and S. T. Wang, *Adv. Mater.*, 2013, **25**, 606-611.
(31) Q. F. Cheng, M. Z. Li, F. Yang, M. J. Liu, L. Li, S. T. Wang and L. Jiang, *Soft Matter*, 2012, **8**, 6740-6743.
(32) D. Wu, S. Z. Wu, Q. D. Chen, S. Zhao, H. Zhang, J. Jiao, J. A. Piersol, J. N. Wang, H. B. Sun and L. Jiang, *Lab Chip*, 2011, **11**, 3873-3879.
(33) Z. J. Cheng, H. Lai, Y. Du, K. W. Fu, R. Hou, N. Q. Zhang and K. N. Sun, *ACS Appl. Mater. Interfaces*, 2013, **5**, 11363-11370.
(34) M. J. Liu, S. T. Wang, Z. X. Wei, Y. L. Song and L. Jiang, *Adv. Mater.*, 2009, **21**, 665-669.
(35) L. Lin, M. J. Liu, L. Chen, P. P. Chen, J. Ma, D. Han and L. Jiang, *Adv. Mater.*, 2010, **22**, 4826-4830.
(36) S. T. Wang and L. Jiang, *Adv. Mater.*, 2007, **19**, 3423-3424.
(37) J. L. Yong, Q. Yang, F. Chen, D. S. Zhang, H. Bian, Y. Ou, J. H. Si, G. Q. Du and X. Hou, *Appl. Phys. A*, 2013, **111**, 243-249.
(38) F. Zhang, W. B. Zhang, Z. Shi, D. Wang, J. Jin and L. Jiang, *Adv. Mater.*, 2013, **25**, 4192-4198.
(40) X. L. Liu, J. Gao, Z. X. Xue, L. Chen, L. Li, L. Jiang and S. T. Wang, *ACS Nano*, 2012, **6**, 5614-5620.
(41) Q. Wen, J. C. Di, L. Jiang, J. H. Yu and R. R. Xu, *Chem. Sci.*, 2013, **4**, 591-595.
(42) M. H. Jin, S. S. Li, J. Wang, Z. X. Xue, M. Y. Liao and S. T. Wang, *Chem. Commun.*, 2012, **48**, 11745-11747.
(43) Q. Zhu, Q. M. Pan and F. T. Liu, *J. Phys. Chem. C*, 2011, **115**, 17464-17470.
(44) F. Chen, D. S. Zhang, Q. Yang, J. L. Yong, G. Q. Du, J. H. Si, F. Yun and X. Hou, *ACS Appl. Mater. Interfaces*, 2013, **5**, 6777-66792.
(45) J. L. Yong, Q. Yang, F. Chen, D. S. Zhang, U. Farooq, G. Q. Du and X. Hou, *J. Mater. Chem. A*, 2014, **2**, 5499-5507.
(46) J. L. Yong, Q. Yang, F. Chen, D. S. Zhang, G. Q. Du, H. Bian, J. H. Si and X. Hou, *RSC Adv.*, 2014, **4**, 8138-8143.
(47) D. S. Zhang, F. Chen, Q. Yang, J. H. Si and X. Hou, *Soft Matter*, 2011, **7**, 8337-8342.
(48) J. L. Yong, F. Chen, Q. Yang, D. S. Zhang, H. Bian, G. Q. Du, J. H. Si, X. W. Meng and X. Hou, *Langmuir*, 2013, **29**, 3274-3279.
(49) J. L. Yong, F. Chen, Q. Yang, D. S. Zhang, G. Q. Du, J. H. Si, F. Yun and X. Hou, *J. Phys. Chem. C*, 2013, **117**, 24907-24912.

(50) D. S. Zhang, F. Chen, Q. Yang, J. L. Yong, H. Bian, Y. Ou, J. H. Si, X. W. Meng and X. Hou, *ACS Appl. Mater. Interfaces*, 2012, **4**, 4905-4912.
(51) F. Chen, D. S. Zhang, Q. Yang, X. H. Wang, B. J. Dai, X. M. Li, X. Q. Hao, Y. C. Ding, J. H. Si and X. Hou, *Langmuir*, 2011, **27**, 359-365.
(52) J. L. Yong, F. Chen, Q. Yang, G. Q. Du, H. Bian, D. S. Zhang, J. H. Si, F. Yun and X. Hou, *ACS Appl. Mater. Interfaces*, 2013, **5**, 9382-9385.
(53) J. L. Yong, Q. Yang, F. Chen, D. S. Zhang, G. Q. Du, H. Bian, J. H. Si, F. Yun and X. Hou, *Appl. Surf. Sci.*, 2014, **288**, 579-583.
(54) F. Chen, H. W. Liu, Q. Yang, X. H. Wang, C. Hou, H. Bian, W. W. Liang, J. H. Si and X. Hou, *Opt. Express*, 2010, **18**, 20334-20343.
(55) S. G. He, F. Chen, K. Y. Liu, Q. Yang, H. W. Liu, H. Bian, X. W. Meng, C. Shan, J. H. Si, Y. L. Zhao and X. Hou, *Opt. Lett.*,2012, **37**, 3825-3827.
(56) T. Her, R. J. Finlay, C. Wu, S. Deliwala and E. Mazur, *Appl. Phys. Lett.*, 1998, **73**, 1673-1675.
(57) M. Y. Shen, C. H. Crouch, J. E. Carey and E. Mazur, *Appl. Phys. Lett.*, 2004, **85**, 5694-5696.

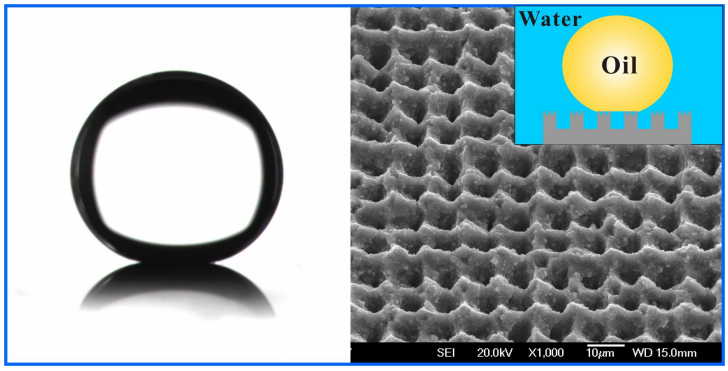

A table of contents entry
A method to fabricate superoleophobic silicon surface with ultralow oil-adhesion by a femtosecond laser.